Modified 4,4′,4″-Tri(N-carbazolyl)triphenylamine as a Versatile Bipolar Host for Highly Efficient Blue, Orange, and White Organic Light-Emitting Diodes

ARTICLE *in* THE JOURNAL OF PHYSICAL CHEMISTRY C · JULY 2012

Impact Factor: 4.77 · DOI: 10.1021/jp3034566

8 AUTHORS, INCLUDING:

Matthew P Aldred
Huazhong University of Science and Technology
48 PUBLICATIONS **884** CITATIONS
SEE PROFILE

Lei Wang
Huazhong University of Science and Technology
301 PUBLICATIONS **6,003** CITATIONS
SEE PROFILE

Jiangshan Chen
Chinese Academy of Sciences
95 PUBLICATIONS **1,780** CITATIONS
SEE PROFILE

THE JOURNAL OF PHYSICAL CHEMISTRY C

Article

pubs.acs.org/JPCC

Modified 4,4′,4″-Tri(*N*-carbazolyl)triphenylamine as a Versatile Bipolar Host for Highly Efficient Blue, Orange, and White Organic Light-Emitting Diodes

Xiao Yang,[†] Hong Huang,[†] Biao Pan,[†] Matthew P. Aldred,[†] Shaoqing Zhuang,[†] Lei Wang,*[,†] Jiangshan Chen,*[,‡] and Dongge Ma[‡]

[†]Wuhan National Laboratory for Optoelectronics, Huazhong University of Science and Technology, Wuhan 430074, P. R. China

[‡]State Key Laboratory of Polymer Physics and Chemistry, Changchun Institute of Applied Chemistry, Graduate School of Chinese Academy of Sciences, Chinese Academy of Sciences, Changchun 130022, P. R. China

ABSTRACT: The hole-transporting material 4,4′,4″-tri(*N*-carbazolyl)triphenylamine (TCTA) is widely used as a host in phosphorescent organic light-emitting diodes (PhOLEDs). Based on the unipolar TCTA, we synthesized a novel bipolar host material, (9-(4-(bis(4-(9*H*-carbazol-9-yl)phenyl)amino)-phenyl)-9*H*-carbazol-3-yl) diphenylphosphine oxide (TCTA-PO) by directly imparting an electron-transporting diphenyl-phosphine oxide moiety to TCTA. It was found that TCTAPO can be used as an ideal versatile host for blue, orange, and white PhOLEDs due to its high triplet energy (E_T = 2.83 eV), high glass transition temperature (T_g = 165 °C), and bipolar charge-transporting ability. The maximum power efficiencies of 40.7 and 43.7 lm/W were achieved in the blue and orange PhOLEDs with FIrpic and $(fbi)_2Ir(acac)$ as the blue and orange dopants, respectively. Furthermore, the single-emitting-layer white organic light-emitting diode (WOLED) based on the emitter of TCTAPO:FIrpic:$(fbi)_2Ir(acac)$ exhibited a maximum current efficiency of 43.7 cd/A, a maximum power efficiency of 47.0 lm/W, and a maximum external quantum efficiency (η_{ext}) of 17.2%. Compared to the PhOLEDs with TCTA as the host, the maximum power efficiencies increased about 56%, 36%, and 81%, for blue, orange, and white devices, respectively.

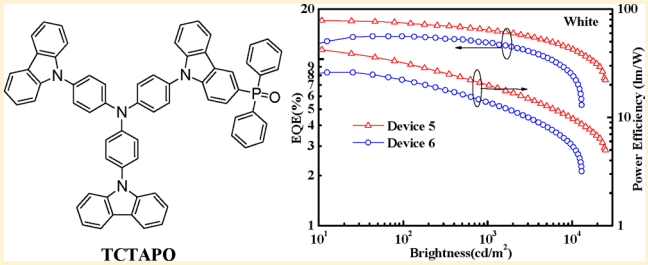

1. INTRODUCTION

Phosphorescent organic light-emitting diodes (PhOLEDs) have attracted much attention because they can achieve 100% internal quantum efficiency by incorporating both triplet and singlet emitters.[1] To date, green and red PhOLEDs with nearly 100% internal quantum efficiency have been successfully achieved,[2] while the development of efficient and stable blue PhOLEDs still remains challenging. On the other hand, white organic light-emitting diodes (WOLEDs) have drawn intensive interests because of their potential application in full-color flat-panel displays and solid-state lighting.[3] In the process of developing OLED lighting, the single-emitting-layer WOLEDs based on a versatile host doped with different color dopants have attracted great interest due to its relatively simple and more cost-effective fabrication processes. In full-phosphor WOLEDs, the host−dopant system has been adopted to improve the device efficiency and reduce the triplet−triplet annihilation. In order to achieve efficient single-emitting-layer full-phosphor WOLEDs, the design of excellent host materials should comply to the following principles: first, the triplet energy (E_T) of the host material must be high enough (≥2.7 eV) to satisfy the blue, green, red, or orange emitter and avoid the energy back transfer to dopants. Second, the highest occupied molecular orbital (HOMO) and the lowest unoccupied molecular orbital (LUMO) of the host materials should match well with the neighboring layers, which could ensure the effective exothermic energy transfer and the confinement of triplet excitons in the emissive layer (EML). It should be noted that if the energy gap (E_g) of the host material is too large, the formation of strong charge traps of dopants would result in high driving voltages and low efficiencies.[4] Finally, the host materials with bipolar charge-transporting property are required to increase the balance of the carriers and broaden the excitons recombination zone, which can improve the device efficiency and reduce the efficiency roll-off.[5] Based on these principles, some versatile bipolar host materials have been reported. For example, Cheng et al. developed a bipolar host material bis-(4-(*N*-carbazolyl)-phenyl)phenylphosphine oxide (BCPO) with a high E_T of 3.01 eV for blue, green, and red phosphorescent devices, and extremely high η_{ext} values of 23.5%, 21.6%, and 17% were achieved in the blue, green, and red PhOLEDs, respectively.[6] Wong et al. reported dimesitylborane/carbazole hybrid bipolar host material CMesB;[7] the devices with CMesB as host showed η_{ext} as high as 20.7% for red, 20% for green, 16.5% for blue, and 15.7% for white at practical brightness, but the maximum power

Received: April 10, 2012
Revised: June 12, 2012
Published: June 20, 2012

   dx.doi.org/10.1021/jp3034566 | *J. Phys. Chem. C* 2012, 116, 15041−15047

Scheme 1. Synthesis of TCTAPO[a]

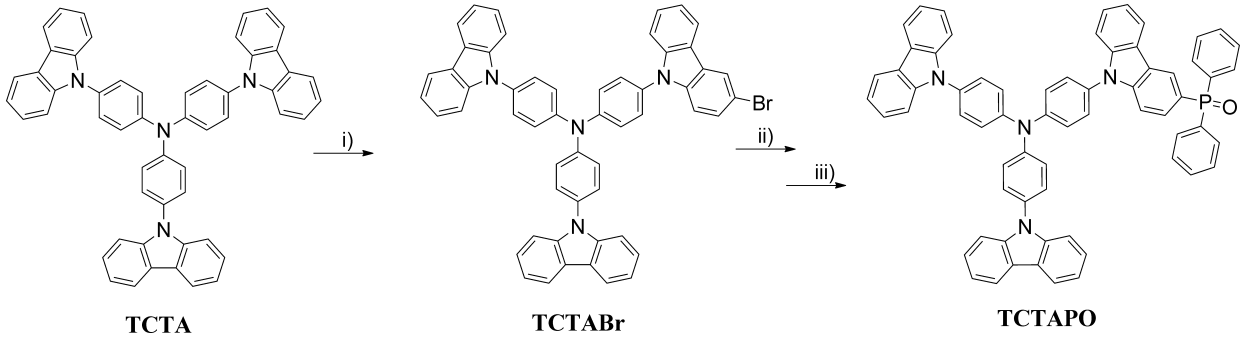

[a]Reaction conditions: (i) NBS, DMF; (ii) chlorodiphenylphosphine, *n*-butyl lithium, THF, −78 °C, N_2; (iii) CH_2Cl_2, H_2O_2, rt, 4 h.

Table 1. Electrochemical, Photophysical, and Thermal Properties of TCTA and TCTAPO

	HOMO (eV)	LUMO (eV)	E_g (eV)	E_T (eV)[a]	abs/PL (nm)[b]	T_d/T_g (°C)
TCTA	−5.09	−1.63	3.46	2.85	238, 293, 326/386	489/152
TCTAPO	−5.3	−1.84	3.46	2.83	293, 327/385, 450	562/165

[a]Measured in CH_2Cl_2 solvent at room temperature. [b]Measured in 2-methyltetrahydrofuran at 77 K.

efficiencies were only 24.5 and 22.6 mL/W in the blue and white devices, respectively. Yang et al. synthesized a silicon-bridged bipolar host *p*-BISiTPA by combining triphenylamine and benzimidazole moiety, resulting in an E_T of 2.69 eV and a T_g of 102 °C. The devices with *p*-BISiTPA as host showed high performance; the η_{ext} values were 16.1%, 22.7%, 20.5%, and 19.1% for blue, green, orange, and white OLEDs, respectively.[8] Although many efforts have been employed, the blue and white devices possessing both high η_{ext} and high power efficiency are still few, and it is still a great challenge to design and synthesize versatile bipolar materials for all-phosphor single-emitting-layer, all-phosphor white OLEDs.

As we know, TCTA has been widely used as a host material for blue, orange, and white PhOLED because of its high morphological stability (T_g = 152 °C) and reasonable triplet energy level (E_T = 2.85 eV).[9] However, the relatively poor device efficiencies at high current density and high efficiency roll-off were often observed, because TCTA only behaves as a hole-transporting type host material with low capability to transport electrons.[10,9b,a] Here, we have introduced an electron-deficient diphenylphosphine oxide group to the TCTA and synthesized a bipolar host material of (9-(4-(bis(4-(9*H*-carbazol-9-yl)phenyl)amino) phenyl)-9*H*-carbazol-3-yl) diphenylphosphine oxide (TCTAPO). The effect of the diphenylphosphine oxide group on the thermal and electrochemical properties, the charge-transporting ability, and the device performance were investigated. It was observed that the efficiencies of the TCTAPO-based devices were much better than those of the TCTA-based devices. When using TCTAPO as the versatile host and FIrpic and $(fbi)_2Ir(acac)$ as the dopants, the maximum power efficiencies can reach 40.7, 43.7, and 47.0 lm/W in the blue, orange, and white PhOLEDs, respectively, which are 1.56, 1.36, and 1.81 times higher than those in the corresponding TCTA-based devices.

2. RESULTS AND DISCUSSION

2.1. Synthesis. The structure and synthetic route of the bipolar host TCTAPO are shown in Scheme 1. TCTA was first brominated selectively using *N*-bromosuccinimide (NBS) in mild conditions. Then the intermediate TCTABr was phosphorylated with chlorodiphenylphosphine, yielding TCTAPO after oxidation with hydrogen peroxide. The intermediate TCTABr was only characterized with mass spectrometry and used directly in the next step reaction without fine purification. Repeated temperature-gradient vacuum sublimation is required for further purification of TCTAPO. The final compound was characterized by ^1H NMR and ^{13}C NMR spectroscopies, mass spectrometry, and elemental analysis.

2.2. Thermal Properties. The thermal stability of the compound TCTAPO was measured by thermal gravimetric analysis (TGA) and differential scanning calorimetry (DSC) under a nitrogen atmosphere, and the related data are listed in Table 1. As shown in Figure 1, the compound TCTAPO exhibits good thermal stability with decomposition temperature (T_d, corresponding to 5% weight loss) at 562 °C in a nitrogen atmosphere. Meanwhile, TCTAPO shows a high glass transition temperature (T_g) of 165 °C in the DSC heating cycle, which is even higher than that of widely used TCTA (152 °C).[11] The high T_g and T_d of TCTAPO can improve the film morphology and reduce the possibility of phase separation upon heating, prolonging the lifetime of the devices.

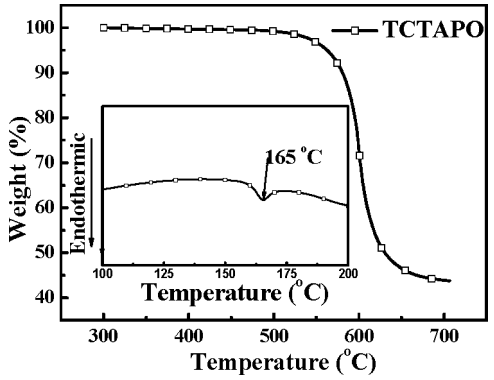

Figure 1. TGA and DSC (inset) curves of TCTAPO recorded at a heating rate of 10 °C/min.

dx.doi.org/10.1021/jp3034566 | J. Phys. Chem. C 2012, 116, 15041−15047

2.3. Photophysical Properties. The UV absorption and PL spectra of TCTAPO and TCTA in dichloromethane are shown in Figure 2. The two compounds exhibit a similar shape

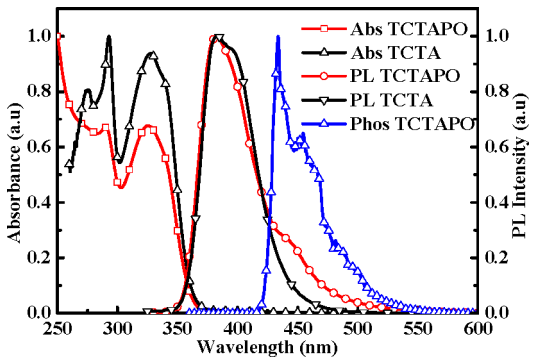

Figure 2. Absorption and emission spectra of TCTAPO and TCTA in dichloromethane at room temperature and phosphorescence spectrum of TCTAPO in 2-methyltetrahydrofuran at 77 K.

absorption spectra, and the absorption peaks at 293 and 327 nm could be assigned to n−π^*, π−π^* transition of triphenyl amine and carbazole, respectively. The absorption edge of the UV/vis spectra of TCTA and TCTAPO is about 358 nm, which corresponds to the band gap at 3.46 eV. The PL emission peak of TCTA in dichloromethane was observed at 385 nm, but for TCTAPO, a new shoulder at 450 nm appeared, which may be ascribed to the energy transfer between TCTA core and diphenylphosphine oxide. The triplet energy of the compound was determined to be 2.83 eV by the highest energy vibronic sub-band of the phosphorescence spectrum in 2-methyltetrahydrofuran at 77 K, which is high enough for the blue phosphor FIrpic (2.65 eV).

2.4. Electrochemical Properties. The electrochemical properties of TCTAPO were investigated by cyclic voltammetry (CV) as shown in Figure 3. The HOMO energy level

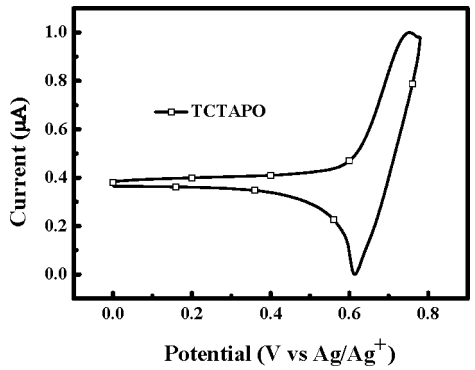

Figure 3. CV curves of TCTAPO. Working electrode, Pt button; reference electrode, Ag/Ag^+. Oxidation CV was performed in dichloromethane containing 0.1 M n-Bu_4NPF_6 as the supporting electrolyte at a scan rate of 100 mV/s.

determined from the onset of the oxidation potential is −5.30 eV using $Ag/AgNO_3$ as the reference electrode (4.7 eV below vacuum), and the LUMO (−1.84 eV) was calculated from the HOMO and energy gap (3.46 eV). Compared to the TCTA (see Table 1), the values of the HOMO and the LUMO were lowered due to the introduction of the electron-withdrawing diphenylphosphine oxide group. The reduction of LUMO energy level will be beneficial for the electron injection from the neighboring layer.

2.5. Quantum Chemical Calculations. To gain insight into the electronic dispersing of the new compound TCTAPO, DFT calculations were performed at the Amsterdam Density Functional (ADF 2009.01). The calculated HOMO and LUMO values are 5.52 and 2.30 eV, respectively. Figure 4 shows HOMO/LUMO distribution and simulated HOMO/LUMO levels of TCTAPO. The HOMO orbital is dispersed over the core triphenyl amine group and the carbazole group, and the LUMO was localized on only the triphenyl amine group. Because there is no direct orbital distribution on the electron-drawing group of diphenylphosphine oxide, the introduction of the electron-deficient group diphenylphosphine oxide only makes the HOMO/LUMO shift to low energy level similarly, and the changes of E_g and E_T are neglectable.

2.6. Electroluminescence. To evaluate the bipolar character of TCTAPO compared to TCTA, the hole-only devices with the structure of ITO/MoO_3 (10 nm)/NPB (40 nm)/host (40 nm)/NPB (40 nm)/Al (100 nm) and the electron-only devices with the structure of ITO/TmPyPB (40 nm)/host (40 nm)/TmPyPB (40 nm)/LiF (1 nm)/Al (100 nm) were fabricated, where NPB is (4,4′-bis[*N*-(1-naphthyl)-*N*-phenylamino]biphenyl) and TmPyPB is (1,3,5-tri(*m*-pyrid-3-yl-phenyl)benzene). NPB and TmPyPB layers were used to prevent electron and hole injection from the cathode and anode, respectively. Figure 5 shows the hole and electron current density of TCTAPO and TCTA. The electron current density of the TCTAPO was higher than that of the TCTA, indicating better electron-injection and -transport properties of the TCTAPO. Meanwhile, the difference of current density between the hole-only and electron-only devices based on TCTAPO is much smaller compared to TCTA at the same voltage, which clearly indicates that TCTAPO is a potential bipolar material capable of transporting electrons and holes by the introduction of the electron-drawing moiety diphenylphosphine oxide.

In view of the high triplet energy (E_T = 2.83 eV) of TCTAPO, a blue electrophosphorescent device using TCTAPO as the host (device 1) was first fabricated; the device structure was ITO/MoO_3 (10 nm)/NPB (40 nm)/TCTAPO (5 nm)/TCTAPO:FIrpic (7 wt %, 20 nm)/TmPyPB (40 nm)/LiF (1 nm)/Al (100 nm). NPB and TmPyPB were used as the hole- and electron-transporting layers, respectively. Pure TCTAPO with thickness of 5 nm was used as the exciton-blocking layer. MoO_3 and LiF served as the hole- and electron-injecting layers, respectively. FIrpic doped into TCTAPO was used as the emitting layer. For comparison, the control device (device 2) with the structure of ITO/MoO_3 (10 nm)/NPB (40 nm)/TCTA (5 nm)/TCTA:FIrpic (7 wt %, 20 nm)/TmPyPB (40 nm)/LiF (1 nm)/Al (100 nm) was also prepared. Figure 6 shows the characteristics of efficiency−brightness and current density−brightness−voltage in the blue PhOLED. The turn-on voltage of 2.7 V was obtained in device 1, and its maximum power efficiency and external quantum efficiency reaches 40.7 lm/W and 17.8%, respectively. At the brightness of 1000 cd/m^2, the high external quantum efficiency is still retained (15.8%). Device 2 exhibits a maximum power efficiency of 26.1 lm/W and a maximum external quantum efficiency of 14.7%, and its turn-on voltage is 3.1 V. The maximum power efficiency in the TCTAPO-based device was increased about 54.6% compared to the TCTA-based device, which can be attributed to the improved charge balance by the bipolar nature of

dx.doi.org/10.1021/jp3034566 | J. Phys. Chem. C 2012, 116, 15041−15047

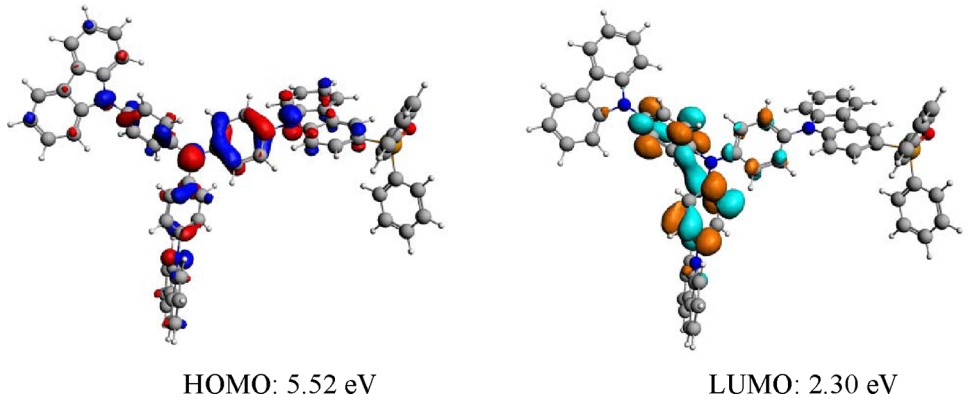

Figure 4. Molecular-orbital surfaces of HOMO and LUMO of the compounds TCTAPO calculated at the DFT//B3LYP/6-31G level.

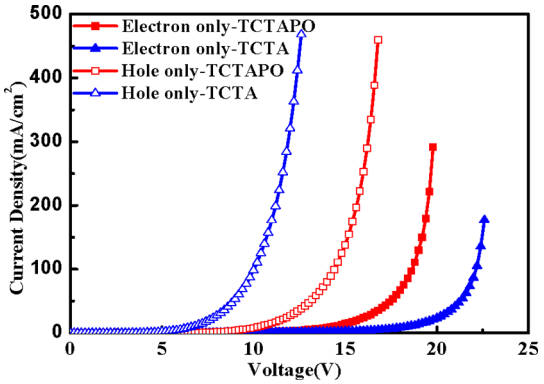

Figure 5. Characteristics of current density–voltage in the hole-only and electron-only devices.

TCTAPO. Additionally, the TCTAPO-based blue device shows the Commission International de l'Eclairage (CIE) coordinates of (0.14, 0.34) from 1 cd/m^2 to 10 000 cd/m^2, corresponding to the emission of FIrpic, which demonstrates that the exciton energy can be efficiently transferred from TCTAPO to FIrpic.

The orange light-emitting devices with the same configuration of ITO/MoO_3 (10 nm)/NPB (40 nm)/TCTAPO (5 nm)/host:$(fbi)_2Ir(acac)$ (7 wt %, 20 nm)/TmPyPB (40 nm)/LiF (1 nm)/Al (100 nm) were fabricated. Similarly, TCTAPO (device 3) and TCTA (device 4) were used as the hosts for comparison. Figure 7 shows the efficiency–brightness and current density–brightness–voltage characteristics of devices 3 and 4. Device 3 shows a low turn-on voltage of 2.75 V, and the maximum external quantum efficiency, current efficiency, and power efficiency are 14.9%, 40.7 cd/A, and 43.7 lm/W, respectively. Device 4 shows a turn-on voltage of 3.0 V and a maximum external quantum efficiency, current efficiency, and power efficiency only of 11.3%, of 31.2 cd/A, and 32.2 lm/W, respectively. The EL spectral of orange device 3 is stabilized and has no visible change even as the luminance increased from 10 to 10 000 cd/m^2, which can be attributed to the efficient limitaion of the excitons recombination in the EML. Here, the maximum power efficiency of device 3 is only increased about 36% compared to device 4, and the current density of the two devices is similar at the same voltage, which could be attributed to the excellent character of electron capture of dopant $(fbi)_2Ir(acac)$.[9b,12]

Encouraged by the impressive results obtained from the blue and orange PhOLEDs, two-color and single-emitting-layer white OLEDs (device 5) were fabricated. The device configuration is ITO/MoO_3 (10 nm)/NPB (40 nm)/TCTAPO (5 nm)/TCTAPO:FIrpic:$(fbi)_2Ir(acac)$ (7 wt %, 0.6 wt %, 20 nm)/TmPyPB (40 nm)/LiF (1 nm)/Al (100 nm). FIrpic and $(fbi)_2Ir(acac)$ were codoped into the bipolar host TCTAPO as EML. Figure 8a and 8b show the efficiency–brightness and current density–voltage–brightness characteristics of device 5; here the white OLED based on TCTA (device 6) was also shown for comparison. It can be seen that the TCTAPO-based white OLED exhibits the peak external quantum efficiency, current efficiency, and power efficiency of 17.2%, 43.7 cd/A, and 47 lm/W, respectively, and its turn-on voltage is only 2.8 V. Remarkably, the white device with TCTAPO as host shows low-efficiency roll-off; its current efficiency slightly decreases from the maximum value of 43.7 to 37.8 cd/A at the brightness of 1000 cd/m^2, and even at the

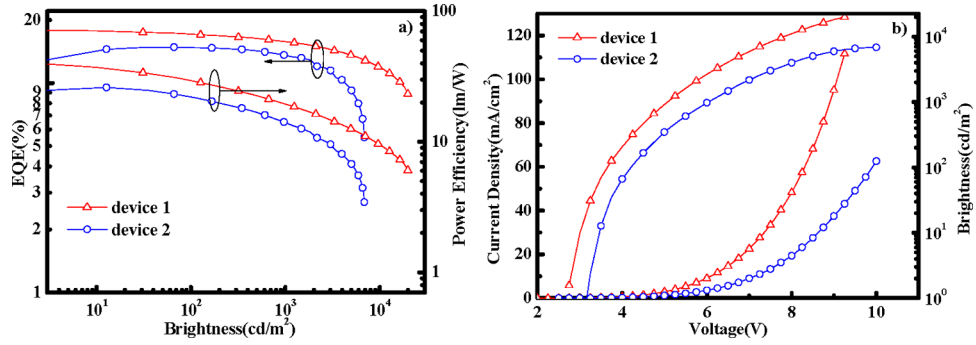

Figure 6. (a) External quantum efficiency (EQE) and power efficiency versus brightness curves. (b) Current density (J)–voltage (V)–brightness (B) characteristics of device 1 and device 2.

dx.doi.org/10.1021/jp3034566 | J. Phys. Chem. C 2012, 116, 15041–15047

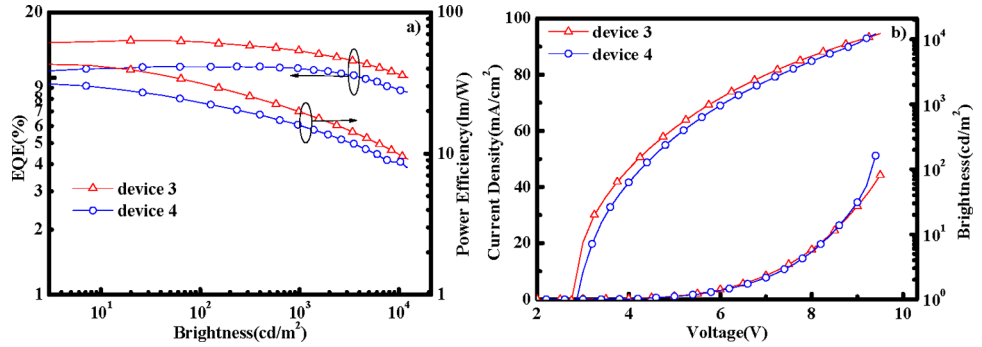

Figure 7. (a) EQE and power efficiency of device 3 (triangle) and device 4 (circle). (b) *J*−*V*−*B* characteristics of different devices.

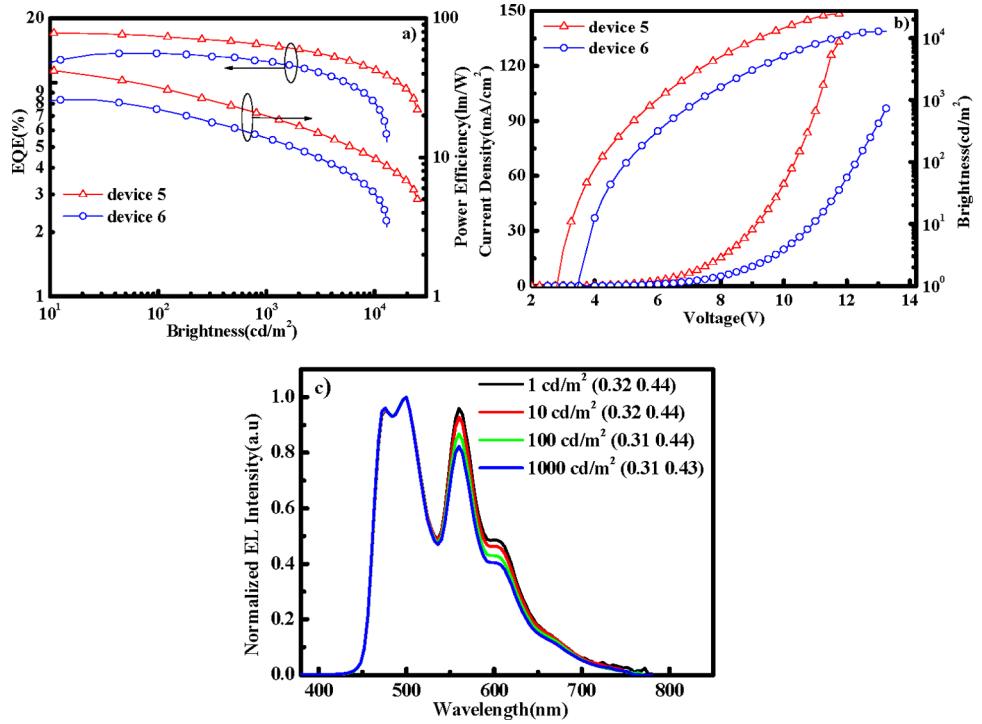

Figure 8. (a) EQE−brightness−power efficiency characteristics of TCTAPO-based white devices. (b) *J*−*V*−*B* characteristics of device 5 and device 6. (c) EL character of WOLED at different brightnesses.

extremely high luminance of 5000 cd/m^2, the current efficiency can still reach 32.4 cd/A. The peak external quantum efficiency, current efficiency, and power efficiency of device 6 are only 13.7%, 35.5 cd/A, and 26.0 lm/W, respectively. The EL spectra of device 5 are shown in Figure 8c; it can be seen that the orange emission decrease weakly with the brightness, but the CIE$_{x,y}$ color coordinates only shift from (0.32, 0.44) at 1 cd/m^2 to (0.31, 0.43) at 1000 cd/m^2 with $\Delta x, y = \pm(0.01,0.01)$.

To further express the impact of the introduction of the electron-transporting biphenylphosphine oxide group to the device performance, the electroluminescence properties of blue, orange, and white PhOLEDs based on TCTA and TCTAPO were summarized in Table 2. It is obvious that the device performances are greatly improved in the blue, orange, and white PhOLEDs when using TCTAPO instead of TCTA as host, which indicates that the bipolar host is more advantageous than the unipolar host for the PhOLEDs.

Table 2. Electroluminescence Properties of the Blue, Orange, and White Devices

device	V_{on} (V)	$\eta_c{}^b$(cd/A)	$\eta_p{}^b$(lm/W)	EQE^b	CIE $(x, y)^c$
1	2.7	35.6, 33.9, 31.0	40.7, 28.4 18.5	17.8, 17.0, 15.6	(0.14, 0.34)
2	3.1	29.7, 29.5, 26.5	26.1, 14.8 13.3	14.8, 14.8, 13.3	(0.14, 0.34)
3	2.8	40.7, 40.0, 35.8	43.7, 31.4, 18.7	14.9, 14.6, 13.1	(0.52, 0.48)
4	3.0	31.2, 31.2, 30.3	32.2, 22.2, 15.3	11.3, 11.2, 11.0	(0.52, 0.48)
5	2.9	43.7, 41.5, 37.8	47.0, 30.7, 20.0	17.1, 16.4, 15.0	(0.31, 0.44)
6	3.4	35.5, 35.2, 31.9	26.0, 21.0, 13.4	13.7, 13.7, 12.5	(0.31, 0.43)

[a]Abbreviations: V_{on}, turn-on voltage; L_{max}, maximum luminance; V, voltage; η_c, current efficiency; η_p, power efficiency; CIE(x, y), Commission International de l'Eclairage coordinates. [b]Order of measured value: maximum, then values at 100 and 1000 cd/m^2. [c]Measured at 100 cd/m^2.

dx.doi.org/10.1021/jp3034566 | J. Phys. Chem. C 2012, 116, 15041−15047

3. CONCLUSIONS

In summary, a new bipolar host material has been designed and synthesized by incorporating biphenylphosphine oxide group into the TCTA molecule. The power maximum efficiencies of blue, orange, and white devices based on TCTAPO were achieved at 40.7, 43.7, and 47.0 lm/W, respectively. Compared to devices based on TCTA, the maximum efficiencies have been improved by about 56% for blue, 36% for orange, and 81% for white. This study could provide a useful strategy in the design of new host materials to satisfy the special criteria required for PhOLEDs.

4. EXPERIMENTAL SECTION

4.1. General Information. All solvents and materials were used as received from commercial suppliers without further purification. ^{1}H NMR and ^{13}C NMR spectra were measured on a Bruker-AF301 AT 400 MHz spectrometer. Elemental analyses of carbon, hydrogen, and nitrogen were performed on an Elementar (Vario Micro cube) analyzer. Mass spectra were carried out on an Agilent (1100 LC/MSD Trap) using ACPI ionization. UV−vis absorption spectra were recorded on a Shimadzu UV−vis−NIR Spectrophotometer (UV-3600). PL spectra were recorded on Edinburgh instruments (FLSP920 spectrometers). Differential scanning calorimetry (DSC) was performed on a PE Instruments DSC 2920 unit at a heating rate of 10 °C/min from 30 to 200 °C under nitrogen. The glass transition temperature (T_g) was determined from the second heating scan. Thermogravimetric analysis (TGA) was undertaken with a PerkinElmer Instruments (Pyris1 TGA). The thermal stability of the samples under a nitrogen atmosphere was determined by measuring their weight loss while heating at a rate of 10 °C/min from 30 to 700 °C. Cyclic voltammetry measurements were carried out in a conventional three-electrode cell using a Pt button working electrode of 2 mm in diameter, a platinum wire counter electrode, and a Ag/$AgNO_3$ (0.1 M) reference electrode on a computer-controlled EG&G Potentiostat/Galvanostat model 283 at room temperature. Reduction CV of all compounds was performed in dichloromethane containing 0.1 M tetrabutylammoniumhexafluorophosphate (Bu_4NPF_6) as the supporting electrolyte. The onset potential was determined from the intersection of two tangents drawn at the rising and background current of the cyclic voltammogram.

4.2. Computational Details. The geometrical and electronic properties were performed with the Amsterdam Density Functional (ADF) 2009.01 program package. The calculation was optimized by means of the B3LYP (Becke three-parameters hybrid functional with Lee−Yang−Perdew correlation functionals)[13] with the 6-31G(d) atomic basis set. Then the electronic structures were calculated at the τ-HCTHhyb/6-311++G(d, p) level.[14] Molecular orbitals were visualized using ADFview.

4.3. OLED Device Fabrication and Measurement. The EL devices were fabricated by vacuum deposition of the materials at a base pressure of 5×10^{-6} torr onto glass precoated with a layer of indium tin oxide (ITO) with a sheet resistance of 25 Ω/square. Before deposition of an organic layer, the clear ITO substrates were treated with oxgen plasma for 5 min. The deposition rate of organic compounds was 0.9−1.1 Å/s. Finally, a cathode composed of LiF (1 nm) and aluminum (150 nm) was sequentially deposited onto the substrate in the vacuum of 10^{-6} torr. The $J-V-B$ of the devices was measured with a Keithley 2400 Source meter and PR655. All measurements were carried out at room temperature under ambient conditions.

4.4. Synthesis of Compounds. Synthesis of *N,N*-bis(4-(9*H*-carbazol-9-yl)phenyl)-4-(3-bromo-9*H*-carbazol-9-yl)-aniline (TCTABr): A mixture of tris(4-(9*H*-carbazol-9-yl)-phenyl)amine(TCTA) (3.7 g, 5.0 mmol) and NBS (0.9 g, 5.0 mmol) in $CHCl_3$ (250 mL) was stirred at room temperature for about 24 h, and then the mixture was washed with water. After the solvent had been completely removed, the white powder residue was harvested (3.8 g). Yield: 94%. MS(APCI): calcd for$C_{54}H_{35}N_4Br$, 818.2; found, 819.0 $(M + 1)^+$.

Synthesis of (9-(4-(bis(4-(9*H*-carbazol-9-yl)phenyl)amino)-phenyl)-9*H*-carbazol-3-yl) diphenylphosphine oxide (TCTA-PO): Under N_2 atmosphere, *n*-butyl lithium (0.44 mL, 1.10 mmol, 2.5 M in hexane) was added slowly to a solution of TCTABr (0.82 g, 1.00 mmol) in THF (80 mL) at −78 °C. After stirring for 2.0 h, solution of chlorodiphenylphosphine (0.22 g, 1.00 mmol) in THF (50 mL) was added and a clear, pale yellow solution appeared. The reaction solution was further stirred for 16 h at room temperature before quenching with 60 mL of water. The mixture was extracted with dichloromethane (100 mL). The combined organic phases were dried ($MgSO_4$) and concentrated under reduced pressure to give a crude compound. The crude material was purified by column chromatography. The white material obtained was dissolved in dichloromethane (50 mL), and to the solution was added 30% aqueous H_2O_2 (20 mL). The mixed solution was stirred for 4 h at room temperature. The organic and aqueous portions in the mixed solution were separated, the aqueous portion was extracted with dichloromethane, and the combined organic layer was dried over $MgSO_4$. The solvent was evaporated, and the product was sublimed at 380 °C to give the desired final product in 52% total yield. ^{1}H NMR ($CDCl_3$, 400 MHz): δ (ppm) 8.60−8.57 (d, J = 12.0 Hz, 1H), 8.17−8.11 (m, 5H), 7.77−7.72 (m, 4H), 7.68−7.63 (m, 1H), 7.59−7.43 (m, 29H), 7.35−7.29 (m, 5H). ^{13}C NMR ($CDCl_3$, 400 MHz): δ (ppm) 147.03, 146.24, 142.90, 141.57, 140.95, 133.97, 133.09, 132.95, 132.26, 132.16, 131.78, 129.44, 129.32, 128.51, 128.39, 128.31, 126.82, 125.95, 125.55, 125.43, 125.31, 125.06, 123.47, 123.38, 122.89, 121.95, 120.86, 120.77, 120.37, 119.99, 110.17, 109.99, 109.85, 109.77. MS (APCI): calcd for $C_{66}H_{45}N_4OP$, 940.3; found, 941.4 $(M + 1)^+$. Anal. Calcd for $C_{66}H_{45}N_4OP$(%): C 84.24, H 4.82, N 5.95, O 1.70, P 3.29; found: C 84.22, H 4.84, N 5.94, O 1.68, P 3.32.

AUTHOR INFORMATION

Corresponding Author

*E-mail: wanglei@mail.hust.edu.cn (L.W.); jschen@ciac.jl.cn (J.C.).

Notes

The authors declare no competing financial interest.

ACKNOWLEDGMENTS

This work was supported by the central allocation grant from Donghu New & High Technology Development Zone, Wuhan Science and Technology Bureau (01010621227) and NSFC/China(21161160442). The Analysis and Testing Centre of the Huazhong University of Science and Technology is acknowledged for characterization of new compounds.

REFERENCES

(1) (a) Helander, M. G.; Wang, Z. B.; Qiu, J.; Greiner, M. T.; Puzzo, D. P.; Liu, Z. W.; Lu, Z. H. *Science* **2011**, *332*, 944−947. (b) Zheng, T.; Choy, W. C. H. *Adv. Funct. Mater.* **2010**, *20*, 648−655. (c) Ikai, M.; Tokito, S.; Sakamoto, Y.; Suzuki, T.; Taga, Y. *Appl. Phys. Lett.* **2001**, *79*, 156−158. (d) Baldo, M. A.; O'Brien, D. F.; You, Y.; Shoustikov, A.; Sibley, S.; Thompson, M. E.; Forrest, S. R. *Nature* **1998**, *395*, 151−154. (e) Huang, W.-S.; Lin, J. T.; Chien, C.-H.; Tao, Y.-T.; Sun, S.-S.; Wen, Y.-S. *Chem. Mater.* **2004**, *16*, 2480−2488. (f) Fan, C. H.; Sun, P.; Su, T. H.; Cheng, C. H. *Adv. Mater.* **2011**, *23*, 2981−2985. (g) Liu, S. W.; Divayana, Y.; Sun, X. W.; Wang, Y.; Leck, K. S.; Demir, H. V. *Opt. Express* **2011**, *19*, 4513−4520. (h) Cho, Y. J.; Lee, J. Y. *J. Phys. Chem. C* **2011**, *115*, 10272−10276.

(2) (a) Kim, D. H.; Cho, N. S.; Oh, H.-Y.; Yang, J. H.; Jeon, W. S.; Park, J. S.; Suh, M. C.; Kwon, J. H. *Adv. Mater.* **2011**, *23*, 2721−2726. (b) Tao, Y.; Wang, Q.; Yang, C.; Zhong, C.; Qin, J.; Ma, D. *Adv. Funct. Mater.* **2010**, *20*, 2923−2929. (c) Tao, Y.; Wang, Q.; Yang, C.; Zhang, Z.; Zou, T.; Qin, J.; Ma, D. *Angew. Chem., Int. Ed.* **2008**, *47*, 8104−8107. (d) Lu, K.-Y.; Chou, H.-H.; Hsieh, C.-H.; Yang, Y.-H. O.; Tsai, H.-R.; Tsai, H.-Y.; Hsu, L.-C.; Chen, C.-Y.; Chen, I. C.; Cheng, C.-H. *Adv. Mater.* **2011**, *23*, 4933−4937.

(3) (a) Yook, K. S.; Jeon, S. O.; Joo, C. W.; Lee, J. Y. *Thin Solid Films* **2010**, *518*, 4462−4466. (b) Lee, S. J.; Seo, J. H.; Kim, J. H.; Kim, H. M.; Lee, K. H.; Yoon, S. S.; Kim, Y. K. *Thin Solid Films* **2010**, *518*, 6184−6187. (c) Chang, C.-H.; Tien, K.-C.; Chen, C.-C.; Lin, M.-S.; Cheng, H.-C.; Liu, S.-H.; Wu, C.-C.; Hung, J.-Y.; Chiu, Y.-C.; Chi, Y. *Org. Electron.* **2010**, *11*, 412−418. (d) Xie, G.; Zhang, Z.; Xue, Q.; Zhang, S.; Luo, Y.; Zhao, L.; Wu, Q.; Chen, P.; Quan, B.; Zhao, Y.; Liu, S. *J. Phys. Chem. C* **2011**, *115*, 264−269.

(4) (a) Lu, M. H.; Weaver, M. S.; Zhou, T. X.; Rothman, M.; Kwong, R. C.; Hack, M.; Brown, J. J. *Appl. Phys. Lett.* **2002**, *81*, 3921−3923. (b) Zhang, M.; Xue, S.; Dong, W.; Wang, Q.; Fei, T.; Gu, C.; Ma, Y. *Chem. Commun.* **2010**, *46*, 3923−3925. (c) Cho, Y. J.; Lee, J. Y. *Chem.—Eur. J.* **2011**, *17*, 11415−11418. (d) Baldo, M. A.; Lamansky, S.; Burrows, P. E.; Thompson, M. E.; Forrest, S. R. *Appl. Phys. Lett.* **1999**, *75*, 4−6.

(5) (a) Chaskar, A.; Chen, H. F.; Wong, K. T. *Adv. Mater.* **2011**, *23*, 3876−3895. (b) So, F.; Kondakov, D. *Adv. Mater.* **2010**, *22*, 3762−3777. (c) Chen, C.-T.; Wei, Y.; Lin, J.-S.; Moturu, M. V. R. K.; Chao, W.-S.; Tao, Y.-T.; Chien, C.-H. *J. Am. Chem. Soc.* **2006**, *128*, 10992−10993. (d) Zheng, T.; Choy, W. C. H.; Ho, C.-L.; Wong, W.-Y. *Appl. Phys. Lett.* **2009**, *95*, 133304−133306. (e) Luo, Y.; Aziz, H. *J. Appl. Phys.* **2010**, *107*, 094510(1)−094510(4). (f) Matsushima, T.; Adachi, C. *Appl. Phys. Lett.* **2008**, *92*, 063306(1)−063306(3).

(6) Chou, H.-H.; Cheng, C.-H. *Adv. Mater.* **2010**, *22*, 2468−2471.

(7) Lin, M.-S.; Chi, L.-C.; Chang, H.-W.; Huang, Y.-H.; Tien, K.-C.; Chen, C.-C.; Chang, C.-H.; Wu, C.-C.; Chaskar, A.; Chou, S.-H.; Ting, H.-C.; Wong, K.-T.; Liu, Y.-H.; Chi, Y. *J. Mater. Chem.* **2012**, *22*, 870−876.

(8) Gong, S.; Chen, Y.; Luo, J.; Yang, C.; Zhong, C.; Qin, J.; Ma, D. *Adv. Funct. Mater.* **2011**, *21*, 1168−1178.

(9) (a) He, G.; Pfeiffer, M.; Leo, K.; Hofmann, M.; Birnstock, J.; Pudzich, R.; Salbeck, J. *Appl. Phys. Lett.* **2004**, *85*, 3911−3913. (b) Wang, Q.; Ding, J.; Ma, D.; Cheng, Y.; Wang, L. *Appl. Phys. Lett.* **2009**, *94*, 103503(1)−103503(3). (c) Erickson, N. C.; Holmes, R. J. *Appl. Phys. Lett.* **2010**, *97*, 083308(1)−083308(3).

(10) Reineke, S.; Lindner, F.; Schwartz, G.; Seidler, N.; Walzer, K.; Lussem, B.; Leo, K. *Nature* **2009**, *459*, 234−238.

(11) Ding, J.; Wang, Q.; Zhao, L.; Ma, D.; Wang, L.; Jing, X.; Wang, F. *J. Mater. Chem.* **2010**, *20*, 8126−8133.

(12) Zhao, Y.; Chen, J.; Ma, D. *Appl. Phys. Lett.* **2011**, *99*, 163303(1)−163303(3).

(13) (a) Lee, C.; Yang, W.; Parr, R. G. *Phys. Rev. B* **1988**, *37*, 785−789. (b) Serena, P. A.; Soler, J. M.; Garcia, N. *Phys. Rev. B.* **1988**, *37*, 8701−8706.

(14) Boese, A. D.; Handy, N. C. *J. Chem. Phys.* **2002**, *116*, 9559−9569.